This article has been accepted for publication in a future issue of this journal, but has not been fully edited. Content may change prior to final publication. Citation information: DOI 10.1109/JSEN.2014.2345576, IEEE Sensors Journal
Vcelak, Jan; Ripka, Pavel; Zikmund, Ales: Long-Range Magnetic Tracking System, IEEE Sens. J. Vol. 15 (2015) 491-496, DOI: 10.1109/JSEN.2014.2345576

Long Range Magnetic Tracking System

Vcelak J.*, Ripka P.**, Zikmund A.*
*CTU-University Center for Energy Efficient Buildings, **CTU - Faculty of Electrical Engineering

***Abstract*—This paper presents a new long-range full 3D magnetic tracking system for horizontal directional drilling (HDD), and describes its performance. The system is able to determine the full 3D mutual position of the receiver with respect to the transmitter. The system presented here belongs to the category of hybrid trackers using an active magnetic ranger, an optical gyro and three micro-machined inclinometers. The gyro is used for dead-reckoning navigation over long distances (up to 2 km), and the magnetic tracking system, consisting of a coil magnetic transmitter and a magnetometer receiver, is used when two drill heads are approaching each other beneath the surface at the assumed meeting point. The functionality of the system was verified for the maximum range of 17m with 1,2m RMS accuracy, and with 0,34m RMS accuracy for the range below 10m.**

***Index Terms*—magnetic tracking, magnetic sensors**

I. Introduction

Trackers generally evaluate the position and the orientation of a cooperating target. Optical trackers are first-choice devices, but they cannot be used underground. The same applies for differential GPS and similar systems that use radio signals. The tracking systems used for Horizontal Directional Drilling (HDD) usually operate using one of the following principles:

Inertial navigation, using dead reckoning for position estimation [1]

Magnetic compasses (with dead reckoning) [1]

Magnetic trackers (with an artificial magnetic source)[12]

Hybrid systems (combinations of various methods)[7]

A *dead-reckoning system* uses angular rate sensors as well as highly accurate accelerometers. The position is integrated in known distance steps. This principle suffers from the limited accuracy of angular rate sensors and accelerometers. Extremely accurate and expensive sensors are necessary for long distance guidance.

Systems with a magnetic compass suffer from the permanent fields created by magnetized objects. Magnetic sensors alone evaluate only orientation, not position. This is because the Earth's magnetic field changes only slowly with position.

Manuscript received February 4, 2013. (Write the date on which you submitted your paper for review.) This work was supported by grant P102/12/2177P102/12/2177 Nanostructured soft magnetic materials for sensors, and by CZ.1.05/2.1.00/03.0091 UCEEB

Magnetic position trackers estimate the spatial position and the orientation of an object, using an artificial magnetic field. Conventional tracking systems use tri-axial source coils, which are excited either by three sine wave currents of different frequencies, or by a sequence of pulses. Tri-axial magnetic sensors (usually induction coils, AMR sensors or fluxgates) are attached to the tracked object, and they measure the magnetic field from the source. Trackers are used in virtual reality, entertainment, and biomechanical studies. They are also used in the drilling and mining industry since they can operate below the surface [1]

Another class of position sensing devices uses passive LC resonant markers. [2]. One excitation coil and multiple detection coils are usually used. The system is able to localize multiple targets that have different resonant frequencies with accuracy below 1 mm for a distance of 100 mm between the marker and the sensor array.

Other systems use two magnetic sources to estimate the position of the drill bit, using a permanent rotary magnet and a single wire flowing by with AC current [4]. These approaches also have limited range and accuracy.

A system consisting of one transmitter coil and an array of receiving coils on the surface was used for navigating the tunneling robot up to 5 m below the ground. Resolution of 1,5 cm was achieved for a 75 m long drill [5]. However, a system of this kind is impractical, as it cannot be used when drilling under lakes or in an urban environment.

Localization of the single ideal magnetic dipole is the most simple inversion problem in magnetometry. The solution is analytical if we know the three components of the magnetic field and the six components of the field gradient at a single point (the gradient tensor is symmetrical, as long as curlB is zero) [6]. Another approach is the STAR method, recently reviewed in[7].

If the source coil is small compared to the distance, it can be considered as a dipole. Its magnetic field decreases with $1/r^3$, and this is the fundamental problem for long-range trackers.

The hybrid system described in [8] fuses data from an inertial navigation system and a magnetic tracker. This approach has high potential. However, the micro-machined angular rate sensors used in [8] have a large bias drift and random walk, and this limits the performance of the whole device for a short operational time.

In [9], we described an implantable magnetic distance measurement system for stomach volume estimation. The system is based on 2 mm diameter transmission and detection

This article has been accepted for publication in a future issue of this journal, but has not been fully edited. Content may change prior to final publication. Citation information: DOI 10.1109/JSEN.2014.2345576, IEEE Sensors Journal

coils, and it works at 3 kHz frequency. The basic accuracy was 1 mm at 5 cm distance and 5 mm at 10 cm distance. We used a tri-axial detection coil to measure the distance for an arbitrary position, [8]. A similar system using AMR sensors is described in [11].

A 3-D fully magnetic tracker with 1 m range was developed to measure distance in any position [12]. The uncertainty caused by noise and interference is below 1 mm, even in a noisy environment. Systematic errors of ±1 cm can be corrected by using a calibration model.

The system uses a compact tri-axial field source and a tri-axial field sensor. The instrument should work in the vicinity of large metal objects that are highly conductive. In order to avoid field distortion due to eddy currents we had to use an excitation frequency less than10 Hz. It is not practical to use a DC field (e.g. from a permanent magnet), as it cannot be distinguished from the Earth's field. For very low frequencies, an induction coil does not have sufficient sensitivity – AMR magneto resistors or fluxgate sensors are necessary. In comparison with the high precision achieved for distance measurements, the uncertainty for the angular parameters (2 position angles and 3 orientation angles) was too high.

This paper is focused on a hybrid guiding system which uses a dead-reckoning method to navigate the drill head over a large distance, and a magnetic position tracker for a precise final approach. The system is used in situations where there are two drill heads approaching from opposite directions, and they should meet at a defined location. The dead-reckoning system fuses data from gyros and inclinometers, while the magnetic tracking system includes an artificial magnetic source and a magnetometer.

II. Hybrid Tracker

System description

The system presented here was developed for precise horizontal underground drilling guidance. When the drilling path is too long (3km and more), drilling is often done from both sides due to limitations of the drill rig torque. The aim is to meet in the middle of the drill trajectory at a defined location. It is a challenging task to steer both drilling heads to the same point and to stop them safely before contact is made (Fig. 1).

Figure 1. Two approaching drilling heads. Drilling has to be securely stopped before the heads touch

Since the shape and the dimensions are strictly limited in the drilling business by the dimension of the drilling aperture, it was necessary to optimize the shape and also the dimensions of the coil to fit into the HDD drill head.

The dead-reckoning method is used to steer the drilling system over a long distance in the first phase (e.g. 2.5km) to reach the approximate meeting point. DRILLGUIDE GST guiding software uses precise orientation data from accelerometers and angular rate sensors, together with a drill-string distance measurement, to perform this task. This information is used by the dead-reckoning algorithm to calculate the position of the drill-head in WGS84 coordinates. The accuracy (3 sigma) of the angular rate sensors used in DRILLGUIDE GST is 0,04 degrees for the azimuth and 0,02 degrees for the pitch. The dead-reckoning system generally suffers from integral error. The maximum position error for a drilling distance of 1000 meter is theoretically less than 69 cm. So, when drilling from two sides for a total product pipe length of 2000 m, the drill heads may pass each other at a maximum distance of 1.38 m at the desired meeting position. For longer total product pipe lengths, the passing distance will increase proportionally (e.g. for 3000 m the maximum passing distance will be 2,07 m).

Due to the limited accuracy of dead reckoning over long distances, precise guidance is taken over by a magnetic tracker when the expected meeting point is reached. The magnetic tracking system estimates the mutual position between the two drill heads – coordinates X,Y,Z (see Figure 2.). The drill path can then be corrected (taking into account the minimum allowed product pipe bending radius) in order to penetrate the drill precisely from the opposite direction. The whole system consists of a coil excitation unit in one drill head, which acts as an artificial magnetic field source. Magnetic sensors are placed in the second drill head – i.e. the magnetometer unit.

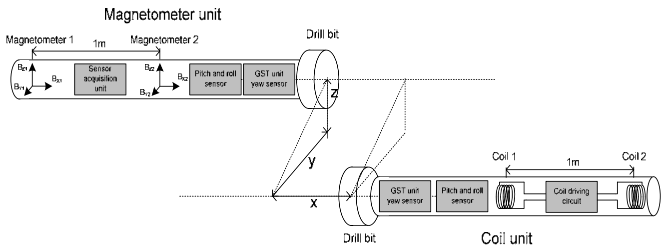

Figure 2. Mutual position of the systems *(x,y,z)*

Figure 3. Transmission and sensing units in the drilling pipes. The shiny pieces are made of AISI 316 non-magnetic alloy.

This article has been accepted for publication in a future issue of this journal, but has not been fully edited. Content may change prior to final publication. Citation information: DOI 10.1109/JSEN.2014.2345576, IEEE Sensors Journal

The **coil unit** consists of two identical axial coils (1000 turns, 10 cm average loop diameter, 12 cm coil length, max current of 30Ap-p). The coil axis is identical with the drill head axis. The coils are excited consecutively with a rectangular shape current (see Figure 6.). The coil excitation unit also contains the control electronics and batteries to provide sufficient excitation power. The distance between the coils is set to 1m in order to have two different magnetic field source locations for each measurement point (Figure 8.). A separate coil driving circuit for each coil allows full excitation current pattern settings (duration as well as amplitude).

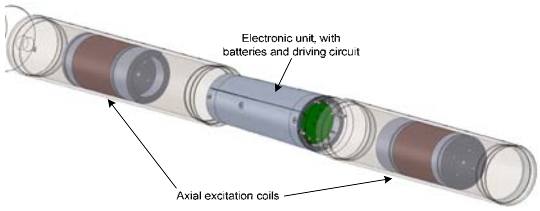

Figure 4. Sketch of the coil unit, two axial excitation coils.

The **magnetometer unit** uses two Billingsley TFM100G2 tri-axial fluxgate sensors with noise of 10 pT/√Hz@1Hz (approximately 100 times better than AMR sensors). The distance between the magnetometers is also set to 1m. Six analog outputs from the magnetometers are processed by 24-bit ADC electronics. The magnetometer unit is also equipped with accelerometer sensors. Good alignment of the magnetic sensors to the accelerometers is necessary, and a special calibration routine was developed for this purpose. The alignment error after calibration is better than 0.1 deg.

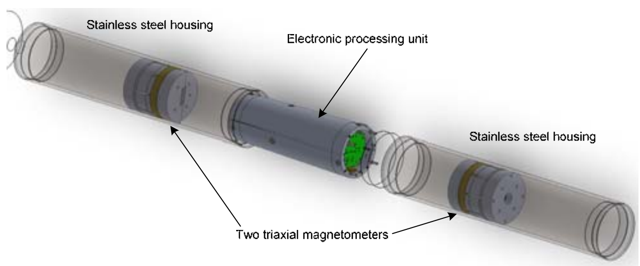

Figure 5. Magnetomter unit sketch, two TFM100G2 magnetometers.

Operation principle

The dead-reckoning algorithm guides the two units to the approximate meeting point at a given location. At this position, the system is switched to magnetic localization mode. In this mode, the two units remain stable, and the precise orientation with respect to the geographical frame is measured. The orientation is described using three angles: azimuth ψ, pitch θ, and roll φ. The precise azimuth value is taken from the optical gyro within the system (the accuracy is better than 0,04deg), the roll and the pitch are taken from the internal accelerometer (accuracy 0,2 deg, after the calibration procedure [13]).

The two downhole units are connected via powerline communication to the uphole receiver. The uphole receiver sends commands to the magnetometer unit to switch to listening mode (to activate the magnetometers) and to the coil unit to apply the excitation sequence to the coils. The excitation sequence is known in terms of the number of excitation pulses, the amplitude and duration, including the synchronization pulse, see Figure 6. The currents for both coils are continuously measured for both current polarities and for both coils. These measured values are communicated to the uphole receiver, and are used to determine the precise magnetic moment difference ΔM between positive I_1^+,and negative I_1^-current polarity for both coils (equation (1)), where N is the number of turns and S is the average area of the turns. The magnetic moment ΔM that is created is used to update the dipole model.

$$\Delta M_1 = N_1 S_1 \left(\frac{I_1^+ - I_1^-}{2}\right) \qquad (1)$$

The magnetometer unit is switched to listening mode when it continuously evaluates the measured signals from all six active axes and searches for the known synchronization pulse pattern in the magnetic data – the mutual correlation principle is used to evaluate the data. The coils are excited by the known and well-defined dual polarity excitation sequence. The pulse duration and also the pulse count are known for each coil. The coils are excited consecutively, one after the other, in order to obtain four independent results. A high current synchronization pulse is sent at the beginning of the excitation sequence. This pulse is used for time synchronization of the two units.

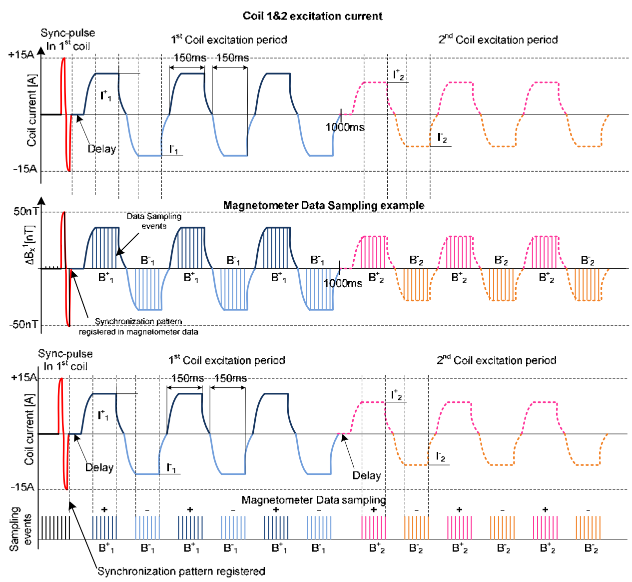

Figure 6. Coil excitation sequence.

The embedded software is able to evaluate the magnetometer signal in real-time for the presence of a synchronization pulse, and can accurately trigger (jitter less than 30ms) the data

This article has been accepted for publication in a future issue of this journal, but has not been fully edited. Content may change prior to final publication. Citation information: DOI 10.1109/JSEN.2014.2345576, IEEE Sensors Journal

sampling procedure. Due to the time synchronization of the units, the magnetic signal data that corresponds to the rising and falling edges of the coil excitation current is skipped in order to avoid any transition effects which might result in inaccurate results. Since the coil excitation current timing pattern is also known on the magnetometer side, the data samples are taken in phase with the excitation pattern. Synchronous detection is therefore then available on the magnetometer side.

Data processing

Both excitation coils are approximated by a dipole with magnetic moment ***M*** and its difference *ΔM* when a dual polarity current is used, equation (1). The magnetic field generated by a dipole in 3D space is described by equation (2), see Figure 7. The radial and tangential components can be described in spherical coordinates using equations (3),(4) where ***r*** is the space point vector, ***φ*** is the angle between the magnetic moment and vector ***r***, and ***M*** is the coil moment caused by current ***I***. The data samples belonging to each positive current amplitude pulse and also to any negative current pulse are evaluated separately to get average values of $\boldsymbol{B}^-_n$ and $\boldsymbol{B}^+_n$.

Due to the dual polarity excitation current and *ΔB* processing, the effect of the ambient static magnetic field caused by hard iron in the close vicinity of the magnetometers, the Earth's magnetic field and also the sensors offsets is suppressed and will not affect the results.

The output value from the magnetometer system is the difference of the measured magnetic field (equation (5)) caused by a positive current pulse and the measured magnetic field caused by the negative current pulse for each magnetometer axis and for both excitation periods, i.e. a total of 12 values (three axes in both magnetometers evaluated for both excitation sequences for coils 1 and 2). These 12 values are communicated to the uphole receiver.

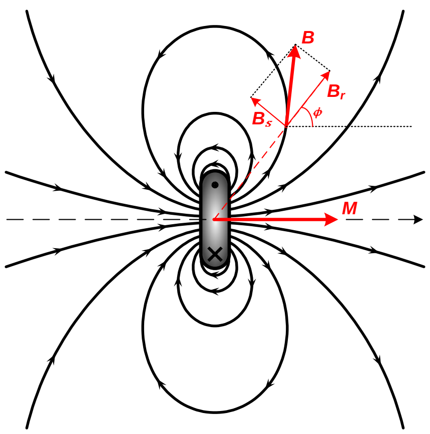

Figure 7. External magnetic field of the dipole.

$$\boldsymbol{B}(\boldsymbol{r}) = \frac{\mu_0}{4\pi}\left(\frac{3\boldsymbol{r}\cdot(\boldsymbol{M}\cdot\boldsymbol{r})}{r^5} - \frac{\boldsymbol{M}}{r^3}\right) \quad (2)$$

$$B_r = \frac{2\mu_0 M \cos\phi}{4\pi r^3} \quad (3)$$

$$B_s = \frac{\mu_0 M \sin\phi}{4\pi r^3} \quad (4)$$

$$\Delta B_{x1} = \frac{B^+_{x1} - B^-_{x1}}{2} \quad (5)$$

The available information from both systems is:

Coil unit

- Ψ_C *coil unit yaw*
- ϑ_C *coil unit pitch*
- φ_C *coil unit roll*
- ΔM_1 *first coil excitation moment*
- ΔM_2 *second coil excitation moment*

Magnetometer unit

- Ψ_M *magnetometer unit yaw*
- ϑ_M *magnetometer unit pitch*
- φ_M *magnetometer unit roll*
- $\boldsymbol{\Delta B}_{1\text{-}1}$ *Magnetic field vector of the differences measured by Magnetometer 1 for the first coil excitation period [nT$_{p\text{-}p}$]*
- $\boldsymbol{\Delta B}_{1\text{-}2}$ *Magnetic field vector of the differences measured by Magnetometer 1 for the second coil excitation period [nT$_{p\text{-}p}$]*
- $\boldsymbol{\Delta B}_{2\text{-}1}$ *Magnetic field vector of the differences measured by Magnetometer 2 for the first coil excitation period [nT$_{p\text{-}p}$]*
- $\boldsymbol{\Delta B}_{2\text{-}2}$ *Magnetic field vector of the differences measured by Magnetometer 2 for the second coil excitation period [nT$_{p\text{-}p}$]*

The key for data processing is to express all magnetic data in coordinates that are related to the coil reference frame. In the coil reference frame we can use equation (2) to describe the magnetic field of the coil. The magnetometer data is transformed to the coil reference frame using matrix equation (6).

$$\boldsymbol{\Delta B}_{[C]} = [D_{\varphi C}][B_{\theta C}][A_{\Psi C}][A_{\Psi M}]^{-1}[B_{\theta M}]^{-1}[D_{\varphi} \quad (6)$$

where ***A,B,D*** are the rotational matrixes for rotation in azimuth, pitch and roll[13]. Index *C* stands for a vector in the coil system reference, and index *M* stands for a vector in the magnetometer system reference.

This article has been accepted for publication in a future issue of this journal, but has not been fully edited. Content may change prior to final publication. Citation information: DOI 10.1109/JSEN.2014.2345576, IEEE Sensors Journal

The iteration algorithm processes the $\Delta\boldsymbol{B}_{[C]}$ vectors to find the estimated 3D position ***R****(x,y,z)* in the space to match the modeled dipole magnetic field. The magnetic field of the dipole is symmetrical with respect to the center of the dipole, and thus the results of the iteration algorithm are not unique. If we have a valid result ***R****(x,y,z)* then result -***R****(-x,-y,-z)* is also valid (Figure 8.). There are at least two different results for each processed vector $\Delta B_{[C]}$. In special cases of the mutual position of the coil and the magnetometer (2nd Gauss position), the group of results is infinite, and we cannot localize units for such a position. In this case, the results from the 2nd Gauss position are not taken into account, and only the other the results are used for estimating the position.

Generally there are four different magnetic vector data items to process and therefore eight possible results (2 magnetometers, 2 coils). The physical mutual displacement of the magnetometers is known (1m), as is the coil 1 and coil 2 displacement (1m). Using this knowledge and all eight possible results from the iteration algorithm, we can rule out results that do not conform with our real geometry. The real results do not overlie each other exactly, due to the presence of noise and sensor inaccuracies.

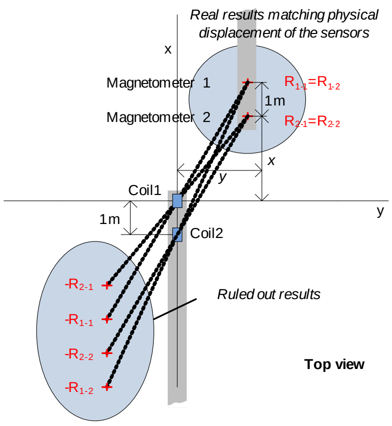

Figure 8. Results of the iteration algorithm.

The final result ***R****(x,y,z)* is then transformed to the operator's reference frame (the locally leveled body reference frame of the coil unit), using equation(7).

$$\boldsymbol{R}' = [\boldsymbol{A}_{\psi C}]^{-1}[\boldsymbol{B}_{\theta C}]^{-1}\left[\boldsymbol{D}_{\varphi C}\right]^{-1} \times \boldsymbol{R} \qquad (7)$$

This recalculated result ***R'*** is presented to the operator in two graphical plots - top view and cross-sectional view.

Results

The system functionality was verified during factory acceptance tests on a group of mutual position measurements. It should be noted that the overall accuracy of the system is influenced by the following factors:

- The overall distance between the coil and the magnetometer unit
- The mutual orientation of the magnetometer unit with respect to the coil unit (There are special orientations where position estimation is not possible)
- The attitude accuracy for estimating the unit yaw, pitch and roll
- The magnetometer sensor accuracy and noise level
- Any soft magnetic objects or material in the close vicinity of the magnetometers

The contribution of various error sources to the final position accuracy is beyond the scope of this paper, but is described in [15]. A complete unit with electronics and coils or magnetometers consists of the outer torque transmission AISI-316 pipe 2m in length, and the inner AISI-316 housing that hermetically seals the magnetometers and coils with electronics. This 2m long non-magnetic piece is a part of the standard drill chain created by the drill bit and other components made from a magnetic steel alloy. The complete system was used for the test measurements in order to be as close as possible to real operation conditions. The real position of the systems was measured and was compared with the calculated results. The overall system accuracy is presented in two ways in accordance with operators' preferences. Figure 9. shows the total position vector error, also counting in the error in the *X* - longitudinal direction - equation (9). For practical use of the system, the error in the *X* direction is not critical for penetrating the opposite drill. We therefore also introduce the YZ error in equation (10). This is calculated only from the position error in Y and Z direction, see Figure 10. The accuracy of the system was calculated for two ranges – close range below 10m, and long range up to 17m. The close range accuracy is 0,34m RMS (±1,17m max) and the long range accuracy is 1,2m RMS (±6,1m max).

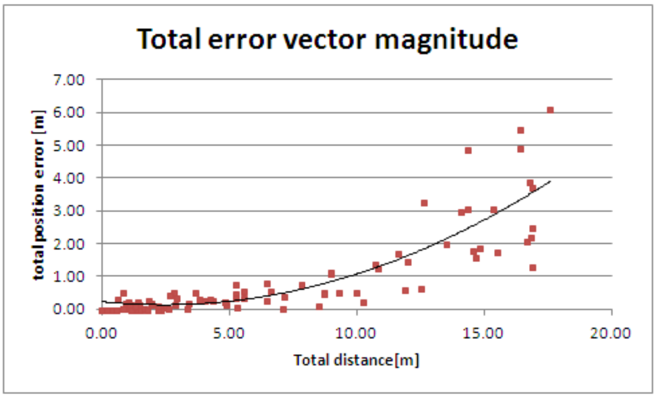

Figure 9. Total error vector magnitude.

This article has been accepted for publication in a future issue of this journal, but has not been fully edited. Content may change prior to final publication. Citation information: DOI 10.1109/JSEN.2014.2345576, IEEE Sensors Journal

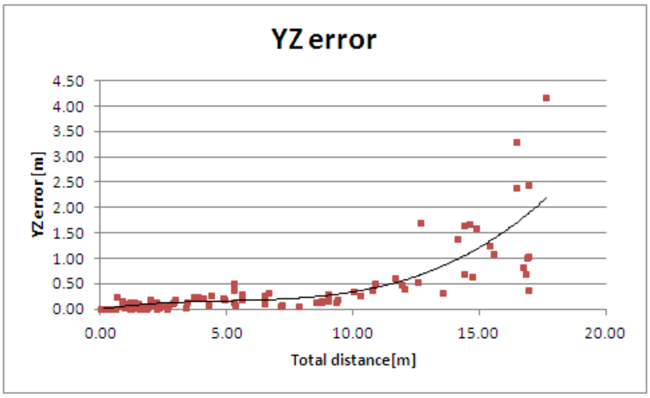

Figure 10. YZ error magnitude, the error in the longitudinal direction is not counted in.

$$\vec{E} = \overrightarrow{R_{real}} - \overrightarrow{R_{calc}} = [X_{err}, Y_{err}, Z_{err}] \quad (8)$$

$$|\vec{E}| = \sqrt{X_{err}^{2} + Y_{err}^{2} + Z_{err}^{2}} \quad (9)$$

$$|\overrightarrow{E_{YZ}}| = \sqrt{Y_{err}^{2} + Z_{err}^{2}} \quad (10)$$

The results presented here were measured in various positions (X in the range of 0 to 17m, Y in the range of 0,2 to 5m, and Z in the range of 0 to 1m) and also in various mutual orientations of both systems. The mutual roll of the system was in the full range of <0°;360°>, while the mutual azimuth was in the range of 180±5° and pitch ±5°. This orientation is used in real applications when drill heads face each other.

III. CONCLUSION

We have developed a full 3D magnetic localization system which is capable of operating in the range of 17m with error better than 1,2m RMS and with accuracy 0,34m RMS for the close range below 10m. In the very close range below 3m, the system is able to localize the second unit with accuracy better than 0,25m RMS, which is well sufficient for proper operation. In cooperation with the gyroscopic navigation device developed by Brownline B.V. under the trade name DRILLGUIDE GST, the complete system is able to operate on drills that are even more than 5km in total length. It has been found that proper sensor placement in the units is critical for accurate localization. The roll alignment of the accelerometer and the magnetic sensors in the magnetometer unit is critical, and the system is therefore calibrated before it is used for the first time. The accelerometer axes are mathematically aligned with the magnetometer axes and also with the longitudinal axis of the system. In the case of the coil excitation system, only the magnetometer is aligned with the longitudinal axis of the system, since the coil placement is accurate and is invariant to the roll position of the coil [13][14].

REFERENCES

[1] AG. Ledroz, Pecht E., Cramer D., Mintchev MP. FOG-based navigation in downhole environment during horizontal drilling utilizing a complete inertial measurement unit: Directional measurement-while-drilling surveying, IEEE TRANSACTIONS ON INSTRUMENTATION AND MEASUREMENT, VOL. 54, NO. 5, OCTOBER 2005

[2] P. Ripka, K. Závěta, Magnetic Sensors: Principles and Applications. In: K.H.J. Buschow, editors: Handbook of Magnetic Materials, Vol 18, Elsevier, 2009, pp. 347-420.ISBN: 978-0-08-054814-2

[3] Hashi S., Masaharu T., S. Yabukami, M. Ohya, K. Ishiyama, Y. Okazaki, and K. I. Arai: Development of Magnetic Motion Capture System for Multi-Position Detection, Sensor Lett. 5, 300–303 (2007)

[4] Tao Liu, Boxiong Wang, Yuanyuan Cui, Jin Zhang. Direction and position measurement in HDD using two magnetic fields. Sensors and Actuators A 185 (2012) 168– 172

[5] Tsujimura T. and Tetsuya M.: Electromagnetic system navigating tunneling robots, Robotics and Autonomous Systems, Volume 40, Issue 4, 30 September 2002, Pages 229-238.

[6] Nara Takaaki, Satoshi Suzuki, and Shigeru Ando: A Closed-Form Formula for Magnetic Dipole Localization by Measurement of Its Magnetic Field and Spatial Gradients, IEEE TRANS. MAGN., VOL. 42, NO. 10, OCTOBER 2006 3291

[7] Y.Sui, G. Li, S. Wang and J. Lin: Asphericity error correction of magnetic gradient tensorinvariants method for magnetic dipole localization, IEEE Trans. Magn. 48 (2012), 4701-4706

[8] H. M. Schepers, D. Roetenberg, P. H. Veltink: Ambulatory human motion tracking by fusion of inertial and magnetic sensing with adaptive actuation, Med Biol Eng Comput (2010) **48**:27–37

[9] Tomek J, Mlejnek P, Janasek V, et al.: Gastric motility and volume sensing by implanted magnetic sensors, Sensor Letters **5** (2007), 276-278

[10] J. Tomek, P. Mlejnek, V. Janásek, P. Ripka, P. Kašpar and J. Chen: The precision of gastric motility and volume sensing by implanted magnetic sensors, Sensors and Actuators A **142** (2008), 34-39.

[11] Liu Y., Y. Wang, D. Yan, Y. Zhou: DPSD Algorithm for AC Magnetic Tracking System, IEEE conf. Virtual Environments Human-Computer Interface and Meas. Syst., (2004), 101-106.

[12] A. Zikmund, P. Ripka: Magnetic Tracker with High Precision, Proc Eurosensors 2011, Procedia Engineering 25 (2011), 1617-1620.

[13] J. Vcelak, “Application of Magnetic Sensors for Navigation Systems”, Shaker Verlag GmbH, Germany (May 29, 2009), ISBN 978-3832277383

[14] J. Včelák, P. Ripka, A. Platil, J. Kubík, P. Kašpar: *Errors of AMR Compass and Methods of Their Compensation*, Sensors & Actuators A, Vol. 129, pages 53-57, 2006

[15] J. Včelák, A. Zikmund, J. Kral: *Long range magnetic localization-accuracy and range study,* SENSORS & THEIR APPLICATIONS XVII Book Series: Journal of Physics Conference Series, Volume: 450, Article Number: 012023 DOI: 10.1088/1742-6596/450/1/012023, 2013